International Journal of Engineering & Technology, 7 (2.7) (2018) 570-576

International Journal of Engineering & Technology

Website: www.sciencepubco.com/index.php/IJET

Research Paper

Indirect Vector Controlled Asynchronous Motor Drive's Dynamic Performance and Analysis with A New Modified MPPT Controller

B. Pakkiraiah[1*], Pallam Paul Ratnakanth [2], Ch. Haribabu [3], O. Chandra Sekhar [4]

[1]Associate Professor, [2,3]M.Tech Research Scholars, [4]Professor, [1,2,3,4]Department of Electrical and Electronics Engineering, [1,2,3,4]Koneru Lakshmaiah Education Foundation Deemed to be University, Greenfields, Vaddeswaram, [1,2,3,4]Guntur, Andhra Pradesh, India-522502.

**Corresponding author E-mail: [1*]pakki1988@gmail.com*

Abstract

Generation of electricity from the PV system has nowadays chosen as a best energy collecting source, due to its abundance availability and also to save the conventional energy sources to the future generation. Because all the conventional sources are coming to an extinct. That is the reason, everybody are looking towards the available renewable energy resources like wind, solar, bio mass, ocean, tidal and geothermal. But, upon those, solar and wind sources are maximum preferred sources, due to their easy availability and easy way of collection of energy. This paper presents a modeling of solar photovoltaic (PV) array with a new modified maximum power point tracking (MPPT) controller, which enhances the PV system performance even at abnormal weather conditions. That the existed MPPT controllers were developed based upon the ideal characteristics of constant irradiance with variable temperature and constant temperature with variable irradiance. To overcome the above problem a practical data is considered for designing of MPPT controller which is based upon variable irradiance. But here, it is developed with the variable irradiance and variable temperature with better performance of the system. The output obtained from the PV with a new modified MPPT is given to the boost converter with an inverter to find the dynamic performance of an indirect vector controlled asynchronous motor drive under different operating conditions. For inverter control, a space vector modulation (SVM) algorithm is used, in which the calculation of switching times is proportional to the instantaneous values of the reference phase voltages. The dynamic performance responses like phasor current, torque and speed of the drive by the new modified MPPT along with SVM controlling technique of the inverter are compared and analyzed with the existed method for different operating conditions.

Keywords: *Indirect Vector Control; Asynchronous Motor Drive; Maximum Power Point Tracking; Space Vector Modulation; Torque Ripple; Total Harmonic Distortion; Variable Irradiance and Variable Temperature.*

1. Introduction

Among the renewable energy sources, the energy through the solar photovoltaic system can be considered the most prerequisite sustainable resource because of ubiquity. However the transfer of energy resulting from photovoltaic conversion remains relatively weak. Therefore the tracking control strategies have to be proposed for the PV system to avoid nonlinear V-I and V-P characteristics of PV module [1-3]. The loss of energy conversion is not only in the PV system also with the loads connected to the PV systems with. The criterion of reducing such loss mainly depends on DC-DC switched mode converters maintaining isolation to the connected load by providing of maximum operating voltage V_{MPP} with the help of a MPPT controller [4-5]. An analog circuitry based MPPT controller with the sliding mode controllers introduced to enhance the output and to get better performance under dynamic conditions have been presented [6-7]. The output voltage is sampled several times to oversample switching frequency ratio. Here, the multiple sampling is used to reduce the phase lag. In multi sampled case PI controller is used for higher controller bandwidths. These techniques are used to limit the more susceptible oscillations [8-9].

A fast and unconditionally stable MPPT is used to achieve the fast dynamic response and stability to obtain the better tracking efficiency. The controller can operate as a voltage source or a current source maintaining stability all across the photovoltaic curve, which is analyzed by using the stability region method [10-11]. The sliding mode MPPT controller is to study the performance on a synchronous SEPIC converter. And its extension to various classes of dc/dc converters has been studied. The dynamic response of a MPP tracker can be improved by constant frequency PWM controller [12-13]. Neural network and fuzzy logic based MPPT controller is implemented to attain the maximum producible power from PV panel to feed boost converter in order to reduce the over shooting, time response and oscillations, in increasing the stability and efficiency of the system [14-15].

Indirect vector controlled asynchronous motor drive is fed with PV MPPT output, DC-DC boost converter and inverter for achieving the better performance in its performance parameters. Harmonic content and switching losses are decreased with the appropriate switching selection [16-17]. The operation of fault tolerant for multilevel i.e.7 level inverter is implemented with the SVM controlled technique. Here, the inverter drives the medium voltage 2.3 KV/2250 hp motor drive using the rotor flux oriented control. The indirect rotor flux oriented control is used for asynchronous motors to achieve good dynamic performance [18-19]. Inverter with SVM controlling technique is the combination of no. of sub hexagons, which are formed with the tip of the resultant space vectors from all six sectors. [20-22].

Output voltage and current distortions are minimized with the help of multi-level inverter (MLI). Power quality can also be improved with the help of 1-ø SVM based CHBMLI at various non ideal

conditions using PV system [23]. The relationship between SVM and carrier based PWM are observed to achieve SVM's performance with the use of carrier based PWM. Common mode injection technique is used in carrier based PWM to develop SVM. Because, SVM technique is the peculiar one, due to which its simplicity and better performance at low modulation. Some times SVM technique becomes difficult to achieve when the number of levels increases [24-25]. Soft computing techniques are implemented to increase the better dynamic and steady state performance [26]. The better improvement in the torque ripple is observed from the particle swarm optimization for an optimal torque control of the motor with the indirect vector control [27]. The comparison of fuzzy and neural network based SVM are introduced to obtain good dynamic responses of the motor drive, as well to increase the PV system performance [28-30]. In this paper, section 2 describes about the modeling of solar PV array. Section 3 illustrates the overview of proposed MPPT algorithm. Section 4 discusses the modeling of asynchronous motor and indirect vector control. Section 5 explains about the SVM control technique. Experimental and simulation result analysis are analyzed in section 6 and the concluding statements are provided in section 7.

2. Solar PV array modeling

Solar energy is converted in electrical energy with imposement of solar radiation on the solar panels due to the phenomenon called 'photo electric effect'[31-33]. Here, 6 panels are grouped together by forming of an array with the pair of 2 series-series and such 3 parallel arrangements for obtaining the maximum optimum output voltage and current. Then the maximum power calculated from the solar panel is calculated by $P_{max} = V_{max} * I_{max}$. Where P_{max} represents the power V_{max} is the MPP or operating voltage and I_{max} is the MPP or operating current. Fig. 1 represents the equivalent circuit of the practical PV cell.

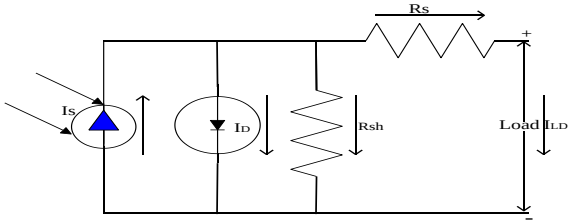

Fig. 1: equivalent circuit of solar PV cell.

$$I_{LD} = I_S - I_D - I_{sh} \quad (1)$$

Where, I_S is the current due to the imposed light and I_D is the diode current, which is calculated as

$$I_D = I_0[\exp\left(\frac{q(V_{LD}+I_{LD}R_S)}{YKT_S}\right) - 1] \quad (2)$$

Where, I_0 the reverse saturation current. By substituting (2) in (1) we get is

$$I_{LD} = I_S - I_0[\exp\left(\frac{q(V_{LD}+I_{LD}R_S)}{YKT_S}\right) - 1] \quad (3)$$

Where, I_{LD} is the module output current.

$$I_S = \frac{G}{G_R}\left(I_{SCR} + \mu_{SCR}\ (T_S - T_{SCR})\right) \quad (4)$$

Here, I_{SCR} refers to the generated current due to photons at reference condition; G, G_R the irradiance, actual and at reference condition respectively, μ_{SCR} is the short circuit temperature coefficient, T_S , T_{SCR} are the solar cell actual and reference temperatures respectively

$$I_O = I_{OR}\left(\frac{T_S}{T_{SCR}}\right)^3 \exp\left[\left(\frac{q\varepsilon_G}{k\,Z}\right)\left(\frac{1}{T_{SCR}} - \frac{1}{T_{CS}}\right)\right] \quad (5)$$

(5) I_{OR} refers to reverse saturation current at reference condition

The photo current I_S of the PV module is linearly proportional to the solar irradiation and available temperature. The module maximum short circuit current 'I_{SCR}' is chosen from the reference data sheet.

3. New modified MPPT controller

Maximum power point tracking controller is used for extracting the optimum power from PV module. Though there are several no. of algorithms to track the MPP efficiently but many of them are working with slow tracking. This is resulting for the low conversion of electrical energy from the panel with poor efficiency. Due to this, the performance of the system also gets reduced. The main purposes of all the MPPTs are to improve the PV system performance also efficiency of the system such as Incremental Conductance (INC), Hill Climbing or Perturbation & Observation (P&O) methods. The partial shading multi peak output curve appearances in the PV system are common, where it is quite difficult to develop the algorithm for the accurate tracking with the multiple and non-linear output curves. 30-40 percent of the solar imposed insolation is used to convert into the electrical output with the normal PV module. That is the reason, to increase the efficiency of the solar power conversion; we incorporate the MPPT controller to the PV system. That the maximum power is obtained only when the source resistance becomes equal to the load resistance. DC-DC boost converter is connected to the PV MPPT output in order to meet the requirement of inverter with SVM controlling technique. This happens due to the continuous monitoring and alteration of the duty cycle to the boost converter as a switching pulse. The proposed new modified MPPT algorithm takes the practical obtained values from the PV array i.e. V, I_L and calculates the maximum tracked available power P_1. This calculated power P_1 is considered as a initial reference value in the algorithm for this iteration. After a time instant 0.01 seconds it takes another set of values V & I_L and calculates P_2. After P_1 and P_2 differential power dp = P_2-P_1 is calculated. This calculated dP is used for the formation of duty cycle D and this can be used for providing of gating pulse for boost converter. For the next iteration P_2 is considered as the initial reference and the process gets repeated as shown in the flow chart given in Fig. 2.

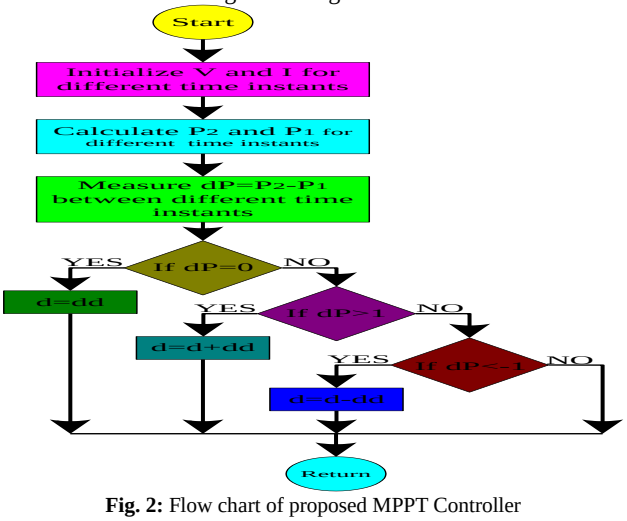

Fig. 2: Flow chart of proposed MPPT Controller

Where dd is the differential duty ratio corresponding to the differential power of particular iteration and d is the duty ratio of the prior time instant. From the proposed MPPT controller it is observed that $I_S >> I_O$ and that the Maximum Power Point current I_{MPP} is also calculated at MPP with thermal voltage as

$$I_{MPP=}I_S - I_O e^{\left(\frac{V_{MPP}}{V_{TH}}\right)} \quad (6)$$

Then I_O becomes as

$$I_O = \frac{I_{SCR}}{e^{\left(\frac{V_{OC}}{V_{TH}}\right)}} \quad (7)$$

With the consideration of V_{OC} and V_{TH} the calculation of I_{MPP} is

$$I_{MPP} = I_{SCR}\left[1 - e^{\left(\frac{V_M - V_{OC}}{V_{TH}}\right)}\right] \quad (8)$$

Then the thermal voltage V_{TH} is calculated as

$$V_{TH} = \frac{V_{MPP} - V_{OC}}{ln\left(\frac{I_{SCR} - I_{MPP}}{I_{SCR}}\right)} \quad (9)$$

So Array power can be calculated as

$$P_{ARRAY} = V_{MPP} \times I_{MPP} = I_S \times V - I_O[e^{\left(\frac{V}{V_{TH}}\right)} - 1] \times V \quad (10)$$

From this by deriving the above equation w.r.t. the voltage we get the maximum array power as

$$P_{ARRAY\ MAX} = \frac{\partial P_{ARRAY}}{\partial V} = I_O\left[e^{\left(\frac{V}{V_{TH}}\right)} - 1\right] + I_O \times \frac{V}{V_{TH}}\left[e^{\left(\frac{V}{V_{TH}}\right)} - 1\right] \quad (11)$$

From above equation we are observing for the maximum voltage that gives the maximum array power is $V=V_{MPP}$. So that

$\frac{\partial P_{ARRAY}}{\partial V}\ at\ V = V_{MPP} = 0$, Then it gives

$$I_{MPP} - \frac{V_{MPP}}{V_{TH}} \times I_D = 0 \quad (12)$$

3.1. PV module practical outputs with the conventional and proposed new modified MPPT controllers

Under Standard Test Conditions, the irradiance provided is 1000 W/m^2 and temperature is about 25^{o}C. During this the results obtained with the existed and new modified MPPT as represented in Fig. 3. Here, that the maximum power point voltage V_{MPP} and current I_{MPP} from the new modified MPPT are observed as 30.7 Volts and 8.13 Amps respectively.

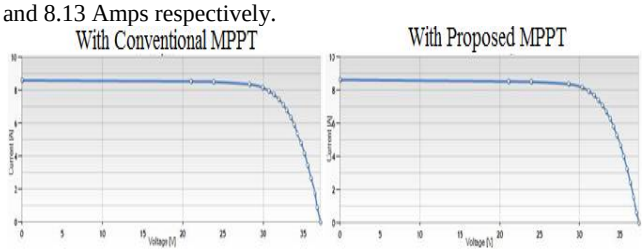

Fig. 3: PV module practical I-V characteristics of with the conventional and new modified MPPT controller

3.2. PV module practical outputs of the new modified MPPT at variable insolation and constant temperature

If the insolation gets varied from 1000 to 100 W/m^2 by maintaining the constant temperature results the linear increment of current and slow increment of voltage till the irradiance rise and decreases with irradiance fall. These results are available in Fig. 4

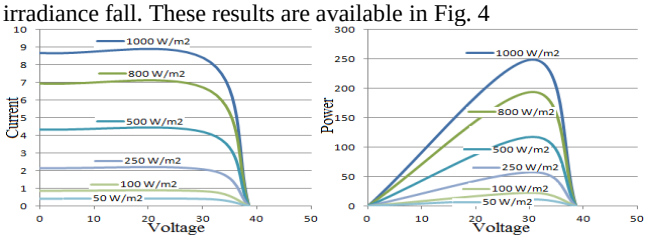

Fig. 4: PV module practical characteristic curves at variable insolation and constant temperature

3.3. PV module practical outputs of the new modified MPPT at variable irradiance and variable temperature

Here, that the temperature and irradiance both are varying, then I there will be a increase of array current and fractional increase of voltage upto the irradiance rise and vice-versa. Similarly, there will be a increase of PV system current and drastic decrease of voltage with the temperature hike and decreases with the same manner. Those outcomes are presented in Fig. 5

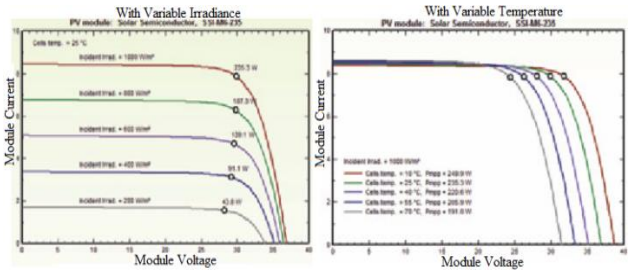

Fig. 5: PV module practical characteristic curves with variable insolation and variable temperature

4. Indirect vector controlled asynchronous motor drive's modeling

The three-ø, squirrel-cage asynchronous motor drive's mathematical modeling with the stator reference frame is illustrated as

$$V_{qs} = (R_S + pL_{sS})i_{qS} + pL_m i_{qR} \quad (13)$$

$$V_{ds} = (R_S + pL_S)i_{dS} + pL_m i_{dR} \quad (14)$$

$$0 = pL_m i_{qS} - \omega_R L_m i_{dS} + (R_R + pL_R)i_{qR} - \omega_R L_R i_{dR} \quad (15)$$

$$0 = \omega_E L_m i_{qS} + pL_m i_{dS} + \omega_R L_R i_{qR} + (R_R + pL_R)i_{dR} \quad (16)$$

Where $\omega_R = \frac{d\theta}{dt}$, $p = \frac{d}{dt}$

V_{dS} and V_{qS} are stator d-q axis voltages respectively. i_{dS}, i_{qS} and i_{dR}, i_{qR} are stator and rotor d-q axis currents respectively. R_S and R_R are stator and rotor resistances. L_S, L_R are the stator and rotor self inductances and L_m is mutual inductance. Stator and rotor flux linkages in-terms of inductances are illustrated as

$$\lambda_{qS} = L_S i_{qS} + L_m i_{qR} \quad (17)$$

$$\lambda_{dS} = L_S i_{dS} + L_m i_{dR} \quad (18)$$

$$\lambda_{qR} = L_R i_{qR} + L_m i_{qS} \quad (19)$$

$$\lambda_{dr} = L_R i_{dR} + L_m i_{dS} \quad (20)$$

Stator reference frame voltages and currents with the transformation matrix presented below.

$$\begin{bmatrix} V_{qS} \\ V_{dS} \\ 0 \\ 0 \end{bmatrix} = \begin{bmatrix} R_S + pL_S & 0 & pL_m & 0 \\ 0 & R_S + pL_S & 0 & pL_m \\ pL_m & -\omega_R L_m & R_R + pL_R & -\omega_R L_R \\ \omega_R L_m & pL_m & \omega_R L_R & R_R + pL_R \end{bmatrix} \begin{bmatrix} i_{qS} \\ i_{dS} \\ i_{qR} \\ i_{dR} \end{bmatrix} \quad (21)$$

The electromagnetic torque 'Te' is given by

$$T_e = \frac{3}{2}\left(\frac{p}{2}\right)\left(\lambda_{qR} i_{dR} - \lambda_{dR} i_{qR}\right) \quad (22)$$

Here, as the rotor flux linkages are aligned in phase to the d-axis resulting the 0 q-axis flux linkages. i.e. λ_{qR}=0 from the equations (20) and (23). Then the electromagnetic torque of motor drive is obtained as

$$T_e = \frac{3}{2}\left(\frac{p}{2}\right)\frac{L_m}{L_R}\left(\lambda_{dR} i_{qS}\right) \quad (23)$$

The adjustments in the stator q- axis current 'i_{qS}' results in controlling of torque with the constant rotor flux linkages 'λ_{dR}'. this leads to λ_{qR}=0 and λ_{dR}=λ_R, then the slip speed of the drive is calculated as

$$\omega_{Sl} = \frac{L_m R_R}{\lambda_R L_R} i_{qS} \quad (24)$$

From the calculated ω_r and ω_{Sl}, that the rotor angle (θ_e) is calculated as

$$\theta_e = \int \omega_e dt = \int (\omega_R + \omega_{Sl}) dt = \theta_R + \theta_{Sl} \quad (25)$$

5. SVM controlled technique for the inverter

SVM control technique is implemented to the inverter control for the minimization of switching sequence operation. Switching losses are also reduced with the implementation SVM for the switching states and their redundancies even though when that is operated at fault conditions. Due to this, each individual phase voltages are generated according to their reference. This is making the SVM technique for the transformation of the 3-ø reference voltages in a rotational space vector representation. This also synthesizes the appropriate switching sequence for the inverter, through it is possible to have the redundancy in the sequence. This technique is implemented to reduce the switching and inverter losses.

In this paper, the two level inverter with SVM is fed with solar linked DC-DC boost converter output to get the better dynamic responses of an asynchronous motor drive. Symmetrical controlled pulses and voltage balancing is maintained with proper switching sequence of the inverter with SVM. This operation helps to have the proper output voltages of an inverter by the transformation of 2-ø to the 3-ø, i.e. the d-q axis quantities are transformed into 3-ø reference voltages with the help of park's transformation. Due to this, that the imaginary switching time periods will have the proportional relationship with the instantaneous phase reference voltages as represented below.

$$T_{uS} = \left(\frac{T_S}{V_{DC}}\right) V_{uS}^{*} \, , T_{vS} = \left(\frac{T_S}{V_{DC}}\right) V_{vS}^{*} \, , T_{wS} = \left(\frac{T_S}{V_{DC}}\right) V_{wS}^{*} \qquad (26)$$

Where, V_{DC} and T_S are the DC link voltage and sampling interval times respectively. The sampling frequency is double to the carrier frequency. Then the maximum, middle and minimum imaginary switching time periods are illustrated with the each sampling intervals as.

$$T_{Max} = Max(T_{u1}, T_{v1}, T_{w1}) \qquad (27)$$

$$T_{Min} = Min(T_{u1}, T_{v1}, T_{w1}) \qquad (28)$$

$$T_{Mid} = Mid(T_{u1}, T_{v1}, T_{w1}) \qquad (29)$$

Then the switching time periods T_1 and T_2 for the active voltage vectors obtained as

$$T_1 = T_{Max} - T_{Mid} \text{ and } T_2 = T_{Mid} - T_{Min} \qquad (30)$$

And the inactive voltage vectors switching time period is deduced as

$$T_z = T_S - T_1 - T_2 \qquad (31)$$

That the zero state time is shared by the T_0 and T_7 with the V_0 and V_7 respectively, and can be calculated as

$$T_0 = K_0 T_Z \qquad (32)$$

$$T_7 = (1 - K_0) T_Z \qquad (33)$$

Various SVM controls are developed with different values of k_o considering from 0 to 1. But, in this SVM, that the zero voltage vector time is shared equally among V_0 and V_7, so its value i.e. k_0 value is considered as 0.5 for proper controlling.

5.1. Indirect vector-controlled motor drive.

Indirect vector-controlled motor drive along with the inverter is as illustrated in Fig. 6. The respective d-axis and q-axis reference currents i_{d1}^{*} and i_{q1}^{*} are measured from flux and torque processor unit and again these are compared with the respective i_{d1} and i_{q1} currents that are generated from the phasor transformation. The error outcomes from the comparison produce the d-q axis voltages with the help of PI controllers and limiters. These voltages are again converted into stationary frame for feeding SVM.

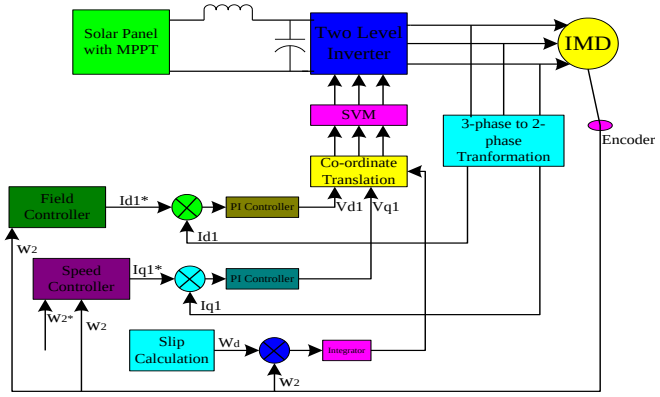

Fig. 6: Vector control of motor with proposed MPPT technique

6. Results and discussion

6.1. PV array theoretical and practical performances with variable irradiance and constant temperatures

When irradiance is considered, then the PV output current and voltages are proportionally increases with respect to the irradiance rise and vice-versa. Comparing to theoretical values practical output values have drooping nature due to variable irradiance for instant to instant. The observations voltage, current and power are available in Fig. 7 (a &b).

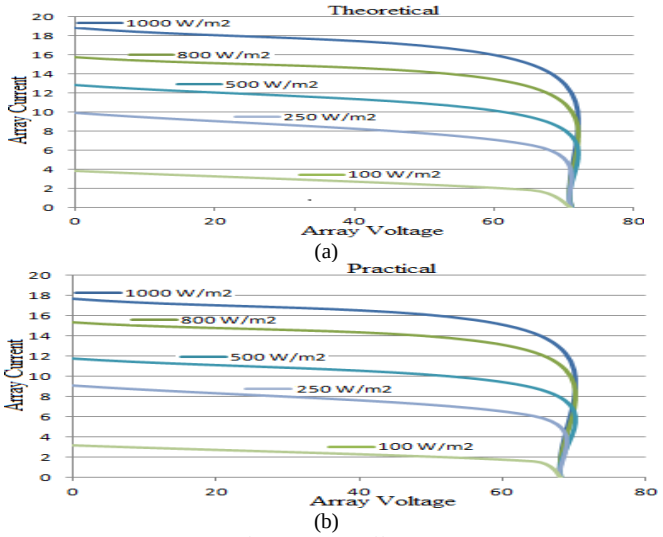

Fig. 7: V-I characteristics of an array at different instants a) Theoretical b) Practical

6.2. PV array theoretical and practical calculated readings with the variable temperature at constant irradiance

With this consideration that the PV array current is linearly increased with the temperature rise and vice-versa. And voltage is drastically decreased and vice-versa. The calculated values with the experimental validation from 8 A.M to 5.30 P.M are illustrated in Fig. 8 (a&b).

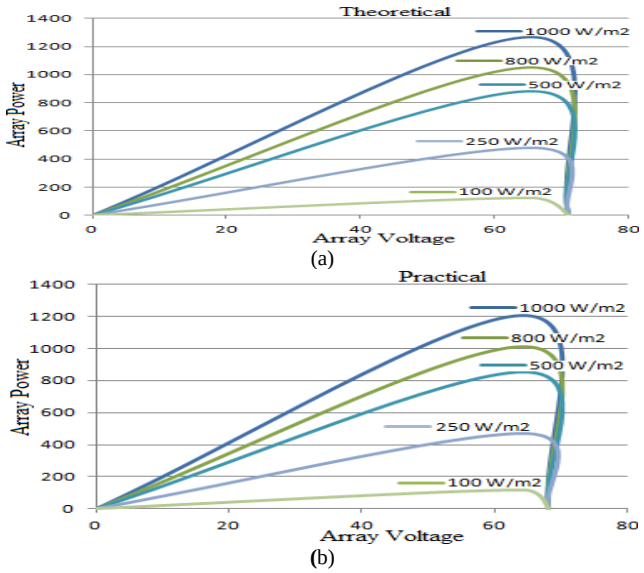

Fig. 8: P-V characteristics of an array at different instants a) Theoretical b) Practical

Table 1: Theoretical and Practical Values of Irradiance, Voltage, Current and Power for Variable Temperature and Irradiance

Time in (am/pm)	Temperature in (^{0}C)	Irradiance in (W/m^2)	Voltage in (Volts)		Current in (Amps)		Power in (Watts)	
			Theoretical	Practical	Theoretical	Practical	Theoretical	Practical
08.00	30.78	145.55	68.04	64.9	3.92	3.53	266.71	229.09
08.30	32.59	290.64	69.42	65.6	7.73	7.03	536.61	461.16
09.06	33.36	413.50	70.16	66.3	10.91	10.04	765.44	723.33
09.30	35.35	480.73	70.47	67.8	12.42	11.7	875.23	793.26
10.00	38.42	499.11	70.53	68.2	12.81	12.16	903.48	829.31
10.30	39.37	518.48	70.62	68.7	13.23	12.63	934.30	867.68
11.00	39.49	559.65	70.76	69.2	14.14	13.6	1000.54	941.12
11.30	40.15	610.10	70.94	69.8	15.35	14.89	1088.92	1039.32
12.00	40.58	636.65	71.20	70.1	15.94	15.54	1134.92	1089.35
12.10	40.71	671.39	71.56	70.4	16.76	16.39	1199.34	1153.85
12.30	41.12	700.60	72.04	71.5	17.27	17.12	1244.13	1224.08
13.00	41.36	729.85	71.62	71.1	17.86	17.72	1279.13	1259.89
13.30	40.52	671.42	71.14	70.8	16.64	16.39	1183.76	1160.41
14.00	40.10	613.13	70.96	69.7	15.49	14.96	1099.17	1042.71
14.30	39.05	557.75	70.78	68.3	14.38	13.59	1017.81	928.19
15.00	38.56	484.56	70.46	67.8	12.55	11.79	884.27	799.36
15.30	37.98	389.05	69.99	67.2	10.13	9.44	708.99	634.36
16.00	37.43	313.32	69.54	65.7	8.39	7.58	583.44	498.06
16.30	37.16	152.91	68.01	64.7	4.16	3.63	282.92	234.86
17.08	33.48	79.63	66.62	63.4	2.18	1.83	145.23	116.02
17.30	32.97	33.84	64.63	62.9	0.87	0.71	56.22	44.65

6.3. Theoretical and practical readings of PV array with the variable irradiance and variable temperature

In practical working conditions, maintaining of constant temperature and irradiance is not possible; these are going to vary from instant to instant. Considering variable irradiance and temperature the following values calculated with the experimental validation from 8 A.M to 5.30 P.M shown in Fig. 9-10.

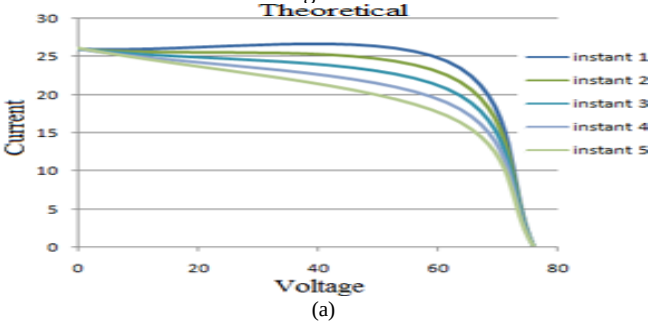

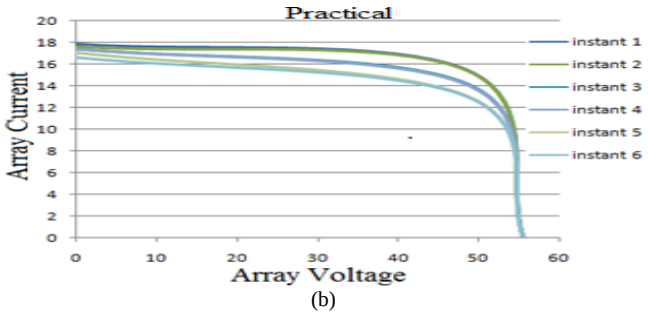

Fig. 9: PV array characteristic curves with variable insolation and variable temperature a) Theoretical b) Practical

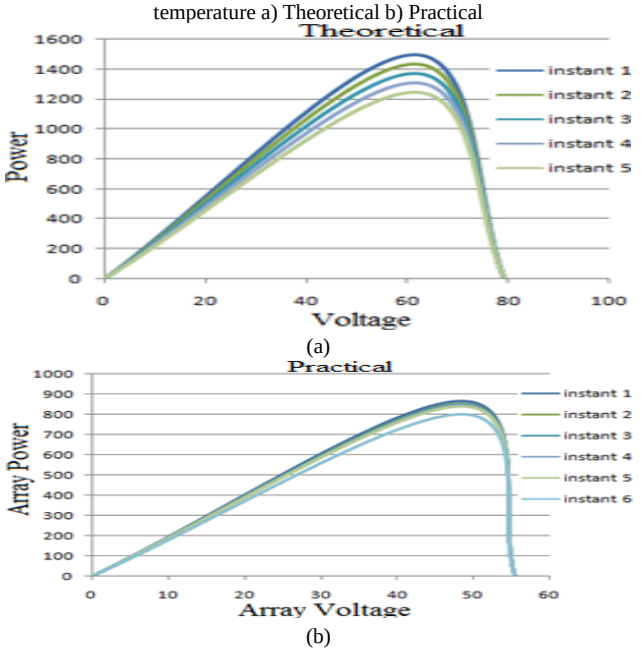

Fig. 10: Array characteristics at variable irradiance and variable temperature a) Theoretical b) Practical

6.4. PV array theoretical and practical validations from proposed MPPT technique

From the proposed MPPT technique it is observed that the maximum theoretical current obtained is 17.86 amps and practical maximum current is about is 17.72 amps at 1:00 pm. Similarly the maximum theoretical voltage and practical voltages are obtained as 71.62 volts and 71.10 volts respectively. And the respective theoretical and practical powers values are validated from the proposed MPPT at 1:00 pm are 1279.13 watts and 1259.89 watts. These validations are taken from morning 8:00 am to evening 5:30 pm; those respective validations are tabulated in the table.1.

6.5. Result analysis of an asynchronous motor drive

Result analysis of the motor drive are observed at different operating conditions by setting the reference speed value to 1300 rpm having of switching frequency 5 KHz. The dynamic performance parameters of drive i.e. current, torque and speed are observed with SVM controlled inverter as depicted in Fig. 11-13.

6.5.1. Performance during starting

That the motor drive's dynamic performances at the starting with the SVM controlled inverter are available from Fig. 11(a), 11(b) and 11(c). As shown in the figures maximum current during the starting is reduced, the ripple contentment in the torque is reduced, drive reaches steady state earlier in case of proposed MPPT controller. The maximum torque obtained with the conventional MPPT is 13.06 N-m where with the new modified MPPT it is 13.80 N-m. Response of the torque gets increases with the modified method. The speed response is reached earlier steady state in the modified method.

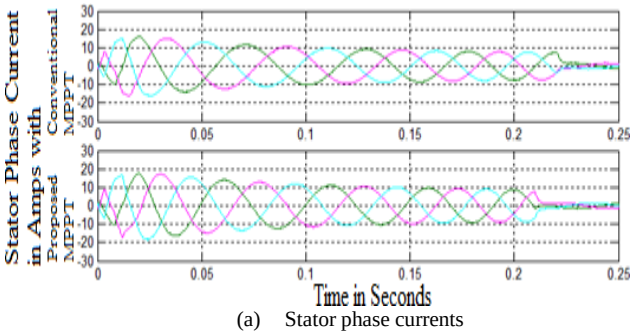

(a) Stator phase currents

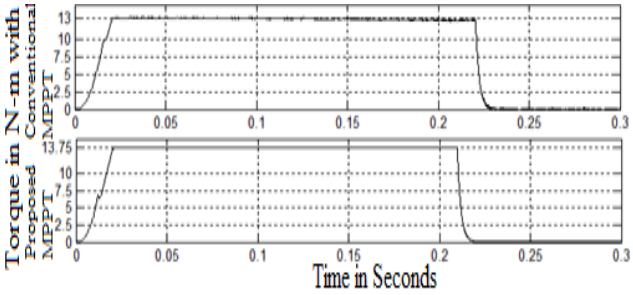

(b) Torque

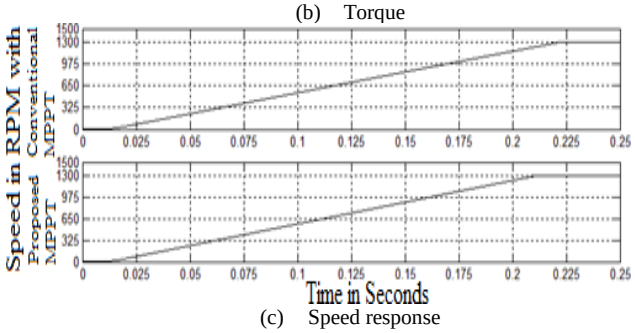

(c) Speed response

Fig. 11: Responses of the motor drive at starting

6.5.2. Performances during steady state

The stator phasor current, speed and torque responses of the motor drive by the SVM controlled inverter during the steady state are illustrated in Fig. 12(a), 12(b) and 12(c). From these results, the torque ripple of the drive with the conventional MPPT and new modified MPPT are found as 0.19 and 0.036 respectively. Lot of ripple quantity is reduced with the new modified method along with the attainment of early steady state speed response.

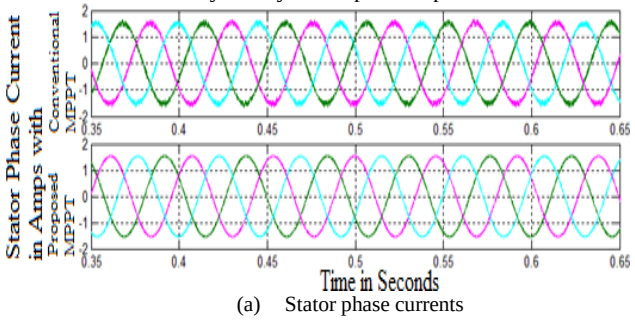

(a) Stator phase currents

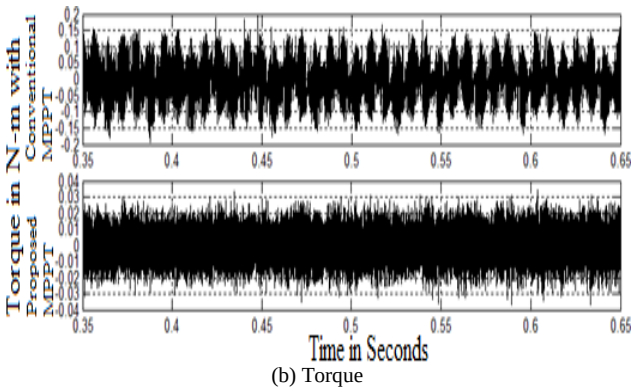

(b) Torque

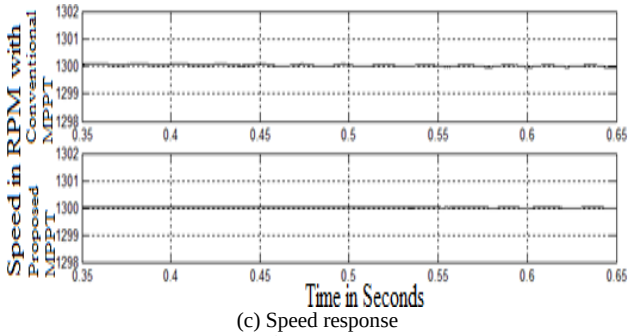

(c) Speed response

Fig.12: Responses of the motor drive at steady state

6.5.3. Reponses of the drive during the transients with step change

Responses of the drive during the transients with the step change operation (the load torque of 8 N-m is applied at 0.7 sec and removed at 0.9 sec) are presented in Fig. 13(a), 13(b) and 13(c). ripple quantity reductions in stator phasor current and torque are further reduced by the involvement of the new modified MPPT and SVM controlled inverter. Also the speed response is reached earlier with the new modified MPPT and SVM controlled inverter.

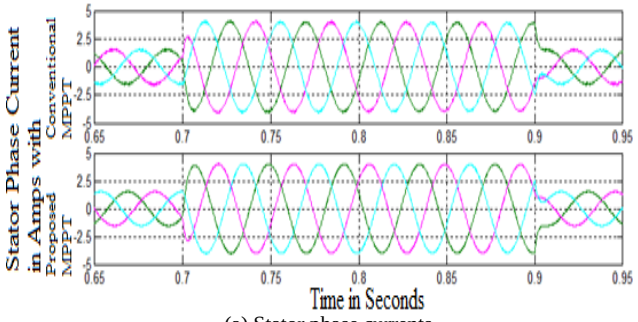

(a) Stator phase currents

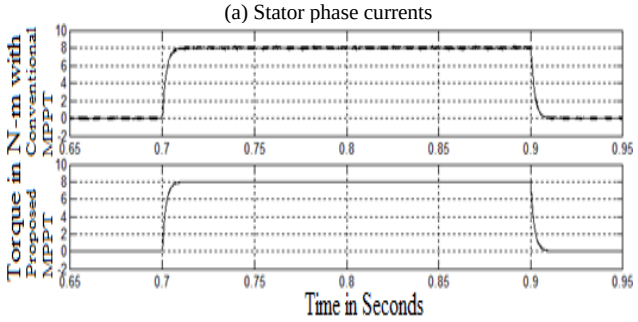

(b) Torque

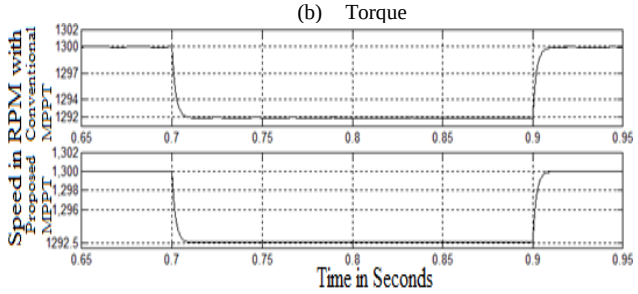

(c) Speed response

Fig.13: Responses of the drive with the transients at step change

7. Conclusions

In this paper, MPPT controller for PV system is worked for the variable irradiance and variable temperature. The responses of the motor drive are compared with the existed and new modified methods with the help of SVM controlled inverter. The theoretical and practical calculations, characteristics are presented for all the worked cases. From those, it is observed that 15-25% variation and improvement is observed compared to the existed methods. From this, that the obtained practical values of MPPT controller are developed to obtain better performance when compared to the conventional

methods.

The proposed MPPT controller calculates the power of a PV system for every 0.01 seconds and gives the more output. It is observed that it gives 10-20% more output with the proposed MPPT under variable irradiance and variable temperature. The better dynamic performance of two-level inverter fed asynchronous motor drive is observed under various conditions with the proposed MPPT. For the inverter control, SVM control technique calculates the symmetrical controlled switching times. Those are proportional to the instantaneous reference phase voltages for the minimization of the sector and angle information. The %THD is reduced to 15-30% compared to with proposed MPPT with the inverter control technique of SVM algorithm compared to conventional based systems.

References

[1] T. P. Sahu and T. V. Dixit, "Modeling and analysis of perturb & observe and incremental conductance MPPT algorithm for PV array using cuk converter", *IEEE Students' Conference on Electrical, Electronics and Computer Science (SCEECS)*, pp.1-6, 2014.

[2] M. A. A. Mohd Zainuri, M. A. Mohd Radzi, Azura Che Soh and N. Abdul Rahim, "Comparative Analysis of the perturb-and-observe and incremental conductance MPPT methods", *IEEE 8th International Symposium on Advanced Topics in Electrical Engineering*, pp.1-1, 2013.

[3] B. Pakkiraiah and G. Durga Sukumar, "Research Survey on Various MPPT Performance Issues to Improve the Solar PV System Efficiency," *Journal of Solar Energy*, vol.2016, no.2016, Article ID 8012432, pp.1-20, 2016. doi:10.1155/2016/8012432.

[4] M. Adly, M. Ibrahim and H. EI Sherif, "Comparative study of improved energy generation maximization techniques for photovoltaic systems", *IEEE Power and Energy Engineering Conference (APPEEC)*, pp.1-5, 2012.

[5] B. Pakkiraiah and G. Durga Sukumar, "Isolated Bi-directional DC-DC Converter's Performance and Analysis with Z-Source by Using PWM Control Strategy," *IEEE 4Th International Conference on Electronics and Communication Systems (ICECS-2017)*, pp.179-183, 2017.

[6] S. Maity and P. Sahu, "Modeling and analysis of a fast and robust module-integrated analog photovoltaic MPP tracker", *IEEE Transactions on Power Electronics*, vol. no.99, pp.1-1, 2015.

[7] B. Pakkiraiah and G. Durga Sukumar, "A New Modified MPPT Controller for Solar Photovoltaic System," *2015 IEEE International Conference on Research in Computational Intelligence and Communication Networks (ICRCICN)*, Kolkata, pp. 294-299, 2015.

[8] M. Bradley, E. Alarcon and O. Feely, "Design-oriented analysis of quantization-induced limit cycles in a multiple-sampled digitally controlled buck converter", *IEEE Transactions on Circuits and Systems I*, vol.61, no.4, pp.1192-1205, 2014.

[9] G. Durga Sukumar and B. Pakkiraiah, "PID controller Tuning using Co-efficient diagram method for indirect vector controlled drive," *Journal of Electrical Engineering and Technology-JEET-Publisher*, vol.12, no.5, pp.1821-1834, 2017.

[10] Y. Levron and D. Shmilovitz, "Maximum power point tracking employing sliding mode control", *IEEE Transactions on Circuits and Systems I*, vol.60, no.3, pp.724-732, 2013.

[11] E. Bianconi, J. Calvente, R. Giral, E. Mamarelis, G. Petrone, C. A. Ramos-Paja, G. Spagnuolo and M. Vitelli, "A fast current based MPPT technique employing sliding mode control", *IEEE Transactions on Industrial Electronics*, vol.60, no.3, pp.1168-1178, 2013.

[12] E. Mamarelis, G. Petrone and G. Spagnuolo, "Design of a sliding mode controlled SEPIC for PV MPPT applications", *IEEE Transactions on Industrial Electronics*, vol.61, no.7, pp.3387-3398, 2014.

[13] B. Pakkiraiah and G. Durga Sukumar, "A New Modified Adaptive Neuro Fuzzy Inference System Based MPPT Controller for the Enhanced Performance of an Asynchronous Motor Drive," *Advancement of Computer Communication & Electrical Technology (ACCET-2016) 21st – 22nd October 2016-Taylor & Francis CRC Press*, pp.349-356, 2017.

[14] N. Khaldi, H. Mahmoudi, M. Zazi and Y. Barradi, "The MPPT control of PV system by using neural networks based on Newton Raphson method", *IEEE International Renewable and Sustainable Energy Conference (IRSEC)*, pp.19-24, 2014.

[15] B. Pakkiraiah and G. Durga Sukumar, "A New Modified Artificial Neural Network Based MPPT Controller for the Improved Performance of an Asynchronous Motor Drive," *Indian Journal of Science and Technology Journal*, vol.9, no.45, pp,1-10, 2016.

[16] J. J. Joshi, P. Karthick and R. S. Kumar, "A solar panel connected multilevel inverter with SVM using fuzzy logic controller", *IEEE International Conference on Energy Efficient Technologies for Sustainability (ICEETS)*, pp.1201-1206, 2013.

[17] M. Aleenejad, H. Iman-Eini and S. Farhangi, "A minimum loss switching method using space vector modulation for cascaded H-bridge multilevel inverter", IEEE *20th International Conference on Electrical Engineering (ICEE)*, pp.546-551, 2012.

[18] M. A. Paymani, M. S. Marhaba and H. Iman-Eini, "Fault-tolerant operation of a medium voltage drive based on cascaded H- bridge inverter", *IEEE Power Electronics Drive Systems and Technologies Conference (PEDSTC)*, pp.551-556, 2011.

[19] K. Pandu Ranga, G. Durga Sukumar, B. Pakkiraiah and M. Subba Rao, "Neuro Fuzzy Based Indirect Vector Control Doubly Fed Induction Generator," *IEEE Seventh India International Conference on Power Electronics (IICPE-2016)*, pp.1-6, 2016.

[20] C. Sreeja and S. Arun, "A novel control algorithm for three phase multilevel inverter using SVM", *IEEE PES Innovative Smart Grid Technologies-India (ISGT India)*, pp.262-267, 2011.

[21] B. Pakkiraiah and G. Durga Sukumar, "A New Modified MPPT Controller for Improved Performance of an Asynchronous Motor Drive under Variable Irradiance and Variable Temperature," *International Journal of Computers and Applications-Taylor & Francis*, pp.1-14, 2016.

[22] A. Mbarushimana and Xin Ai, "Real time digital simulation of PWM converter control for grid integration of renewable energy with enhanced power quality", *IEEE Electric Utility Dereglation and Restructing and Power Technologies (DRPT)*, pp.712-718, 2011.

[23] A. Panda, M. K. Pathak and S. P. Srivastava, "An improved power converter for standalone Photovoltaic system", *IEEE Indian Conferene (INDICON)*, pp.1-6, 2013.

[24] Wenxi Yao, Haibing Hu and Zhengyu Lu, "Comparisons of space-vector modulation and carrier-based modulation of multilevel inverter", *IEEE Transactions on Power Electronics*, vol.23, no.1, pp.45-51, 2008.

[25] B. Pakkiraiah and G. Durga Sukumar, "A Modified MPPT Controller for Indirect Vector Controlled Induction Motor Drive with Variable Irradiance and Variable Temperature in Interfacing with dSPACE DS-1104," *Journal of Electrical Engineering and Technology-JEET-Publisher*, vol.12, no.5, pp.1921-1934, 2018.

[26] Minglei Zhou, Kekang Wei, Chenchen Wang, Xiaojie You, Jian Wang and Liwei Zhang, "A rotor flux oriented scheme of induction machine based on voltage controller", *IEEE Industrial Electronics and Applications*, pp.744-748, 2010.

[27] Dong Hwa Kim, "GA-PSO based vector control of indirect three phase asynchronous motor", *Elsevier Science Direct Applied Soft Computing*, vol.7, no.2, pp.601-611, 2007.

[28] Durga Sukumar, Jayachandranath Jitendranath, Suman Saranu, "Three-level Inverter-fed Asynchronous motor Drive Performance Improvement with Neuro-fuzzy Space Vector Modulation", *Electrical Power Components and Systems*, vol.42, no.15, pp.1633-1646, 2014.

[29] B. Pakkiraiah and G. Durga Sukumar, "Performance and Analysis of an Asynchronous Motor Drive with a New Modified Type-2 Neuro Fuzzy Based MPPT Controller Under Variable Irradiance and Variable Temperature," *Sensors & Transducers-IFSA S.L*, vol.209, no.2, pp.35-44, 2017.

[30] B. Pakkiraiah and G. Durga Sukumar, "Enhanced Performance of an Asynchronous Motor Drive with A New Modified Adaptive Neuro Fuzzy Inference System Based MPPT Controller in Interfacing with dSPACE DS-1104," *International Journal of Fuzzy Systems-Springer* Publisher, vol.19, no.6, pp.1950-1965, 2017.

[31] "Kolluru V R, Mahapatra K and Sudbudhi B, Real-Time Digital Simulation and Analysis of Sliding Mode and P&O MPPT Algorithms for a PV System, International Journal of Emerging Electric Power SystemsVolume 16, Issue 4, 1 August 2015, Pages 313-322."

[32] Kolluru V R, Mahapatra K and Sudbudhi B, Development and implementation of control algorithms for a photovoltaic system, Students Conference on Engineering and Systems, SCES 2013, Article number 6547525.

[33] Kolluru V R, Sarode S S, Patjoshi R K, Mahapatra K and Sudbudhi B, Design and implementation of an optimized sliding mode controller and compared with a conventional MPPT controller for a solar system, WSEAS Transactions on Systems and Control Volume 9, Issue 1, 2014, Pages 558-565